Interface-Dependent Spin-Reorientation Energy Barrier in Fe/MgO(001) Thin Film

Heechae Choi, Eung-Kwan Lee, Sung Beom Cho, Dong Su Yoo, and Yong-Chae Chung, *Member, IEEE*

***Abstract*—Using the density-functional-theory-based atomic modeling, the stable interface structure and the resultant magnetocrystalline anisotropy (MCA) of the Fe/MgO(001) for magnetic random access memory have been studied. The most stable surface structure of Fe/MgO(001) thin-film system was found to be either defect free or possessing oxygen vacancies in a $c(2 \times 1)$ periodicity. The formation of the oxygen vacancies in $c(2 \times 1)$ periodicity on MgO(001) surface reduced the MCA of Fe layer from 1.38 to 0.31 meV/atom. The reduced MCA is originated from the filling of the minority states of the Fe orbital below Fermi level.**

***Index Terms*—Density functional theory, Fe/MgO(001), interface structure, perpendicular magnetic anisotropy.**

I. Introduction

MAGNETOCRYSTALLINE ANISOTROPY (MCA) of ferromagnetic thin films crucially determines various features of magnetic recording devices such as "write" or "read" error rates, power consumption, and thermal stability of the stored information [1]–[3].

Fe layers on a rock salt MgO(001) surface has attracted many researchers due to its tunneling magnetoresistance (TMR) and its applications to memory storage [4]–[10]. Since minimization of the MCAs of Fe/MgO(001) systems allows low energy consumption for "writing" through the Fe/MgO/Fe junctions, there have been various methods to control the MCAs of Fe/MgO(001) system, e.g., applications of external electric fields in vertical direction or the heat-assisted recording [8]. As the system size shrinks, perpendicular MCA of Fe/MgO(001) is utilized in memory storage these days [3], [4]. In Fe/MgO(001) based on using perpendicular MCA the interface structures of the Fe/MgO(001) also contribute to the changes in the MCA [9]–[11]. Recently, density-functional-theory-based theoretical works have successfully predict and explain the interface-dependent magnetic properties of Fe/MgO(001) systems [12], [13]. For instance, Ke *et al.* [12] successfully revealed that the contribution of oxygen vacancy (OV) to the TMR value reduction is strongly dependent on the OV position. On the other hand, Yang predicted that the excess and deficiency of oxygen at the interface enhances and decreases the interlayer exchange coupling of Fe/MgO/Fe(001) system [13].

Motivated by the significance of the Fe/MgO(001) system in memory technologies and recent reports about magnetism control using the interface electronic structure, we performed a DFT study on Fe/MgO(001) to find the most stable interface structure made by OV formations and the effects of atomic structures on the MCA of Fe layer.

II. Calculation Methods

DFT calculations were performed using the Vienna ab initio simulation package code [14]. The plane-wave basis set was expanded to a cutoff energy of 500.00 eV. The projector-augmented waves [15] and the generalized gradient approximation were used [16].

To obtain the most stable atomic structures of MgO(001) and Fe/MgO(001) surface with OVs, six monolayers of rock salt structure MgO slabs with one OV in the periodicities of $c(1 \times 1)$, (1×1), $c(2 \times 1)$, (2×1), $c(2 \times 2)$, (2×2), $c(3 \times 1)$, (3×1), and $c(4 \times 1)$ were prepared with a 20-Å vacuum spacer above the cells. The structural relaxations were performed with k-point grids of $8 \times 8 \times 1$ generated by the Monkhorst–Pack scheme [17]. For the noncollinear magnetism calculations including the spin–orbit coupling term, a careful convergence test was done with k-point grids from $8 \times 8 \times 1$ to $16 \times 16 \times 1$.

III. Math

To study the structure-dependent magnetic properties of Fe on MgO(001), we first obtained the surface phase diagrams of MgO(001) and Fe/MgO(001) systems (Fig. 1). The surface Gibbs free energies were obtained using the following equation:

$$\Delta\gamma(T,P) = \frac{1}{A}\left(G^{\mathrm{surf}}_{\mathrm{slab}}(T,P,N_V) - G^{\mathrm{ref}}_{\mathrm{slab}}(T,P) + N_V\mu_0(T,P)\right). \quad (1)$$

Here, $G^{surf}_{slab}(T,P,N_V)$ and $G^{ref}_{slab}(T,P)$ are the Gibbs free energies of the slab with a certain number of vacancies, N_V, and a reference slab, respectively. T and P are the variable temperature and pressure, respectively. The value of $\Delta\mu_0$ was determined in fully relaxed surface structures. Since we consider only the OV formation in this study, we plotted the surface Gibbs free energy as the function of oxygen chemical potential, μ_0 at fixed temperature and pressure (Fig. 1). Extrapolations

Manuscript received May 29, 2011; revised June 8, 2011; accepted June 14, 2011. Date of publication July 25, 2011; date of current version August 24, 2011. This work was supported by the National Research Foundation of Korea (NRF) grant funded by the Korea government (MEST) No. 2011-0016945. The review of this letter was arranged by Editor L. Selmi.

The authors are with the Department of Materials Science and Engineering, Hanyang University, Seoul 133-791, Korea (e-mail: heechae@gmail.com; gaius@hanyang.ac.kr; csb444@hanyang.ac.kr; dongsuyoo@hanyang.ac.kr; yongchae@hanyang.ac.kr).

Color versions of one or more of the figures in this letter are available online at http://ieeexplore.ieee.org.

Digital Object Identifier 10.1109/LED.2011.2160148

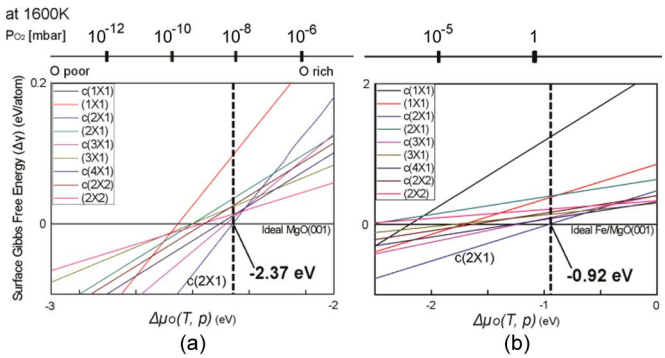

Fig. 1. Surface free energies ($\Delta\gamma$) of (a) MgO(001) and (b) Fe-covered MgO(001) as the functions of the oxygen chemical potential, which is obtained with (1). In the top x-axis, the chemical potential $\Delta\mu_O$ has been translated to the pressure scale bars for the fixed temperature, 1600 K, according to (2). The OVs are formed at $\Delta\mu_O(T,p) = -2.37$ eV and $\Delta\mu_O(T,p) = -0.92$ eV on bare MgO(001) and Fe/MgO(001) surfaces, respectively, both in $c(2\times 1)$ periodicity.

to other temperature and pressure conditions in which surface OVs are formed can be obtained using the equation

$$\Delta\mu_O\left(T, P_{O_2}\right) = \frac{1}{2}\left(\tilde{\mu}(T, P^0) + k_B T \ln\left(\frac{P_{O_2}}{P^0}\right)\right) \quad (2)$$

in which P^0 is the pressure of a reference state and the temperature dependence of the oxygen chemical potential is tabulated in thermodynamical reference [18]. The upper bound is set to be half of the total energy of the isolated oxygen gas molecule so that the oxygen atoms would not condense. In the surface phase diagram, the upper bound of $\Delta\mu_{O2}$ was defined as zero, by using the equation

$$\Delta\mu_0 = \mu_0 - \frac{1}{2}E_{O_2}. \quad (3)$$

Using the formation energy of MgO

$$E_f = \left|E_{\mathrm{MgO}} - E_{\mathrm{Mg}} - \frac{1}{2}E_{O_2}\right|. \quad (4)$$

The allowed range of $\Delta\mu_0$ was given by

$$-E_f \le \Delta\mu_0 \le 0. \quad (5)$$

IV. Results and Discussion

The calculated $-E_f$ for the rock salt MgO with theoretically obtained lattice constant, i.e., 4.19 Å (0.47% smaller than the experimental measurement), was 6.08 eV. As shown in Fig. 1, the most stable equilibrium surface structures of MgO(001) and Fe/MgO(001) were found to be either defect free or with OV on the top surface layer in $c(2\times 1)$ periodicity for both of the systems. The OV formations occur when $\Delta\mu_0$ is below -2.37 and -0.92 eV in MgO(001) and Fe/MgO(001) systems, respectively. In other words, the formation of $c(2\times 1)$ OV row is energetically stabilized when Fe layer is adsorbed.

The perpendicular MCA was defined with the equation

$$MCA = E[\rightarrow] - E[\uparrow] \quad (6)$$

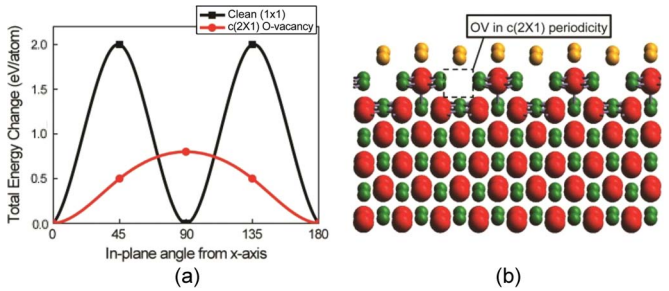

Fig. 2. (a) Total energy changes with the in-plane magnetization rotations of the Fe monolayer on the clean MgO(001) and the $c(2\times 1)$ OV possessing MgO(001). (b) Side view of the Fe/MgO(001) with the $c(2\times 1)$ OVs. The yellow, green, and red spheres represent the Fe, Mg, and O atoms, respectively.

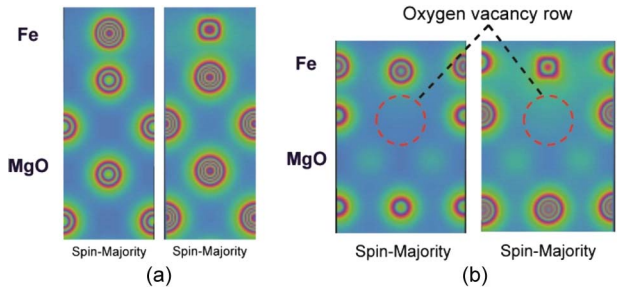

Fig. 3. Charge densities of Fe on (a) clean MgO(001) and (b) the $c(2\times 1)$ OV possessing MgO(001).

where $E[\rightarrow]$ and $E[\uparrow]$ are the total energies of the Fe/MgO(001) system with in-plane magnetization and surface-normal magnetization. Hence, the total energy changes of the defect-free Fe/MgO(001) and the O-deficient Fe/MgO(001) were plotted against the in-plane magnetization angle rotations to find the most stable in-plane magnetization directions of the two systems [Fig. 2(a)]. On the defect-free MgO(001) surface, the stable in-plane magnetization comes every 90° ([100] and [010] directions). However, the magnetization in [100] and [010] directions becomes nonequivalent by the formation of the OV row on the MgO(001) surface [Fig. 2(b)]. According to the energy plot against the in-plane spin rotation angle, the in-plane magnetic easy axis of Fe layer is along the OV row direction (90°) on the oxygen-deficient MgO(001).

The calculated perpendicular MCA of the Fe layer on defect-free MgO(001) surface was 1.38 meV per atom, which agrees well with the previous ab initio study by Niranjan *et al.* [19]. On the $c(2\times 1)$ OV possessing MgO(001) surface, the perpendicular MCA was calculated to be 0.31 meV per Fe atom. The reduced MCA means easier switching of the magnetic easy axis of Fe. Since the ideal MCA of ferromagnetic layer which can resist thermal fluctuation is reported to be 1.2 eV [19], the 0.31 meV/atom is still high compared to the sizes of fabricated MTJ system [20]. This difference (78% reduction) is larger than that obtained from the external electric field application [21].

To see how the MCA of Fe layer on the O-deficient MgO(001) was reduced, the charge distributions (Fig. 3) and the electronic density of states (DOS) were obtained (Fig. 4). The charges of both the spin-majority and the spin-minority states in the defect-free Fe/MgO(001) are localized in the Fe layer [Fig. 3(a)]. The Fe atoms adsorbed on the OV row

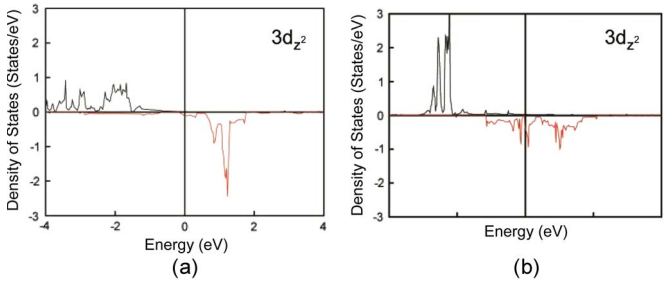

Fig. 4. $3d_{z2}$-orbital DOS of Fe on (a) clean MgO(001) and (b) the $c(2 \times 1)$ OV possessing MgO(001) surface.

have significant amount of spin-minority charge spreading toward the OV site while the Fe atoms on the oxygen on top had similar charge distribution with the clean Fe/MgO(001) case [Fig. 3(b)]. The calculated magnetic moment of Fe on the defect-free MgO(001) was 3.10 $\mu_{\rm B}$. On the O-deficient MgO(001), Fe on the top of an oxygen atom has almost the same magnetic moment with Fe on defect-free MgO(001), i.e., 3.09 μB. However, Fe on OV has reduced magnetic moment, i.e., 2.80 μB.

As can be seen in the Fe DOS, the difference in the MCAs by the OV formation was found to come from the hybridization of Fe spin-minority $3d$-orbital electrons with the underlying OV (Fig. 4). The Fe on defect-free MgO(001) has delocalized spin-majority states and localized spin-minority states only above Fermi level [Fig. 4(a)]. The spin-minority states populate only above Fermi level. All of the $3d$-orbitals of Fe on oxygen on top had similar DOS shapes with Fe on clean MgO(001) surface. However, by the hybridization of spin-minority $3d$-orbital electron of Fe on OV row, some of the spin-minority Fe electron states are shifted below Fermi level [Fig. 4(b)], which reduces the net magnetization from the Fe $3d$-orbital. The smaller magnetic moment of Fe on OV (2.80 $\mu_{\rm B}$) also results from the hybridization of spin-minority Fe $3d$-orbital. Here, it is noticeable that the $3d_{z2}$-orbital contribution to the Fe/MgO(001) MCA control by the interface OV formation is different from the electric field case, where the reductions in the $3d_{\rm yz}$ or the $3d_{\rm yz}$-orbital occupation contribute to the changed MCA value [21].

V. Conclusion

Through the DFT study on the effects of interface structure on the Fe/MgO MCA, we have found that the formation of the OVs on the MgO(001) surface significantly reduces the MCA value (1.38–0.31 meV/atom). The surface phase diagrams of MgO(001) and Fe/MgO(001) show that the $c(2 \times 1)$ periodicity OV row is the most stable surface pattern in ultrahigh vacuum conditions. The spin realignment of Fe layer along the OV row originates from the filling of the spin-majority states of the Fe $3d_{z2}$-orbital below the Fermi energy.

References

[1] M. N. Khan, J. Henk, and P. Bruno, "Anisotropic magnetoresistance in Fe/MgO/Fe tunnel junctions," *J. Phys.: Condens. Matter*, vol. 20, no. 15, p. 155 208, Apr. 2008.

[2] E. Chen, D. Apalkov, Z. Diao, A. Driskill-Smith, D. Druist, D. Lottis, V. Nikitin, X. Tang, S. Watts, S. Wang, S. A. Wolf, A. W. Ghosh, J. W. Lu, S. J. Poon, M. Stan, W. H. Butler, S. Gupta, C. Mewes, T. Mewes, and P. B. Visscher, "Advances and future prospects of spin-transfer torque random access memory," *IEEE Trans. Magn.*, vol. 46, no. 6, pp. 1873–1878, Jun. 2010.

[3] T. T. Maruyama, Y. Shiota, T. Nozaki, K. Ohta, N. Toda, M. Mizuguchi, A. A. Tulapurkar, T. Shinjo, M. Shiraishi, S. Mizukami, Y. Ando, and Y. Suzuki, "Large voltage-induced magnetic anisotropy change in a few atomic layers of iron," *Nat. Nanotechnol.*, vol. 4, p. 158, 2009.

[4] T. Nozaki, Y. Shiota, M. Shiraishi, T. Shinjo, and Y. Suzuki, "Voltage-induced perpendicular magnetic anisotropy change in magnetic tunnel junctions," *Appl. Phys. Lett.*, vol. 96, no. 2, p. 022 506, Jan. 2010.

[5] W. H. Butler, X.-G. Zhang, T. C. Schulthess, and J. M. MacLaren, "Spin-dependent tunneling conductance of Fe|MgO|Fe sandwiches," *Phys. Rev. B, Condens. Matter*, vol. 63, no. 5, p. 054 416, Feb. 2001.

[6] J. Mathon and A. Umerski, "Theory of tunneling magnetoresistance of an epitaxial Fe/MgO/Fe(001) junction," *Phys. Rev. B, Condens. Matter*, vol. 63, no. 22, p. 220 403(R), Jun. 2001.

[7] S. S. P. Parkin, C. Kaiser, A. Panchula, P. M. Rice, B. Hughes, M. Samant, and S.-H. Yang, "Giant tunnelling magnetoresistance at room temperature with MgO (100) tunnel barriers," *Nat. Mater.*, vol. 3, no. 12, pp. 862–867, Dec. 2004.

[8] D. Weller and A. Moser, "Thermal effect limits in ultrahigh-density magnetic recording," *IEEE Trans. Magn.*, vol. 35, no. 6, pp. 4423–4439, Nov. 1999.

[9] C. Tiusan, M. Sicot, M. Hehn, C. Belouard, S. Andrieu, F. Montaigne, and A. Schuhl, "Fe/MgO interface engineering for high-output-voltage device applications," *Appl. Phys. Lett.*, vol. 88, no. 6, p. 062 512, Feb. 2006.

[10] S. Yuasa, T. Nagahama, A. Fukushima, Y. Suzuki, and K. Ando, "Giant room-temperature magnetoresistance in single-crystal Fe/MgO/Fe magnetic tunnel junctions," *Nat. Mater.*, vol. 3, no. 12, pp. 868–871, Dec. 2004.

[11] C.-G. Duan, J. P. Velev, R. F. Sabirianov, W. N. Mei, S. S. Jaswal, and E. Y. Tsymbal, "Tailoring magnetic anisotropy at the ferromagnetic/ferroelectric interface," *Appl. Phys. Lett.*, vol. 92, no. 12, p. 122 905, Mar. 2008.

[12] Y. Ke, K. Xia, and H. Guo, "Oxygen-vacancy-induced diffusive scattering in Fe/MgO/Fe magnetic tunnel junctions," *Phys. Rev. Lett.*, vol. 105, no. 23, p. 236 801, Dec. 2010.

[13] H. X. Yang, M. Chshiev, A. Kalitsov, A. Schuhl, and W. H. Butler, "Effect of structural relaxation and oxidation conditions on interlayer exchange coupling in Fe|MgO|Fe tunnel junctions," *Appl. Phys. Lett.*, vol. 96, no. 26, p. 262 509, Jun. 2010.

[14] G. Kresse and J. Furthmüller, *Vienna Ab-initio Simulation Package*. Vienna, Austria: Univ. Wien, 2001.

[15] G. Kresse and D. Joubert, "From ultrasoft pseudopotentials to the projector augmented-wave method," *Phys. Rev. B, Condens. Matter*, vol. 59, no. 3, pp. 1758–1775, Jan. 1999.

[16] J. P. Perdew, J. A. Chevary, S. H. Vosko, K. A. Jackson, M. R. Pederson, D. J. Singh, and C. Fiolhais, "Atoms, molecules, solids, and surfaces: Applications of the generalized gradient approximation for exchange and correlation," *Phys. Rev. B, Condens. Matter*, vol. 46, no. 11, pp. 6671–6687, Sep. 1992.

[17] H. J. Monkhorst and J. D. Pack, "Special points for Brillouin-zone integrations," *Phys. Rev. B, Condens. Matter*, vol. 13, no. 12, pp. 5188–5192, Jun. 1976.

[18] D. R. Stull and H. Prophet, *JANAF Thermochemical Tables, Natl. Bur. Stan. (U.S.)*, 2nd ed. Washington, DC: U.S. GPO, 1971.

[19] J. Hafner, "Ab initio density-functional calculations in materials science: From quasicrystals over microporous catalysts to spintronics," *J. Phys.: Condens. Matter*, vol. 22, no. 38, p. 384 205, Sep. 2010.

[20] D. C. Worledge, G. Hu, D. W. Abraham, J. Z. Sun, P. L. Trouilloud, J. Nowak, S. Brown, M. C. Gaidis, E. J. O'Sullivan, and R. P. Robertazzi, "Spin torque switching of perpendicular TaICoFeBIMgO-based magnetic tunnel junctions," *Appl. Phys. Lett.*, vol. 98, no. 2, p. 022 501, Jan. 2011.

[21] M. K. Niranjan, C.-G. Duan, S. S. Jaswal, and E. Y. Tsymbal, "Electric field effect on magnetization at the Fe/MgO(001) interface," *Appl. Phys. Lett.*, vol. 96, no. 22, p. 222 504, May 2010.